Available online at www.sciencedirect.com

ScienceDirect

Mendeleev Commun., 2018, **28**, 401–403

Mendeleev Communications

Synthesis and magnetic properties of the exchange-coupled $SrFe_{10.7}Al_{1.3}O_{19}$/Co composite

Evgeny A. Gorbachev,*[a] Lev A. Trusov,[b] Anastasia E. Sleptsova,[a] Evgeny O. Anokhin,[a] Dmitri D. Zaitsev,[b] Alexander V. Vasiliev,[b] Artem A. Eliseev[a] and Pavel E. Kazin[b]

[a] *Department of Materials Science, M. V. Lomonosov Moscow State University, 119991 Moscow, Russian Federation. Fax: +7 495 939 0998; e-mail: gorbachevgenij@gmail.com*

[b] *Department of Chemistry, M. V. Lomonosov Moscow State University, 119991 Moscow, Russian Federation*

DOI: 10.1016/j.mencom.2018.07.020

The magnetic composite $SrFe_{10.7}Al_{1.3}O_{19}$/Co was synthesized by ethylene glycol reduction of cobalt ions on the surface of hexaferrite particles dispersed in the solvent. The resulting material contained magnetically hard submicron hexaferrite particles covered by soft magnetic cobalt nanoparticles. The composite demonstrated the exchange-coupling effect between hard and soft magnetic phases.

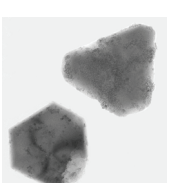

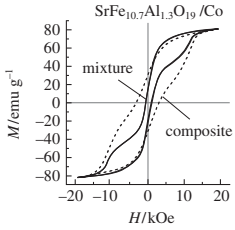

High costs and relatively narrow working conditions of rare-earth magnets force researchers to look for alternative materials with high maximum energy product $(BH)_{max}$.[1–6] Exchange-coupled magnetic composites (ECC) are the two-phase materials, which consist of hard and soft magnetic phases coupled with each other by exchange interactions. In theory of ECC, the hard phase provides a large coercivity and the soft one transmits a high magnetization, thus, magnetic anisotropy of the hard phase aligns spontaneous magnetization of the soft phase. Due to the exchange-coupling effect, the composites display higher $(BH)_{max}$ values than the single hard and soft phases separately. However, both phases have to be structured at the nanoscale in order to achieve the effective coupling.[2–6]

M-type hexaferrites ($BaFe_{12}O_{19}$ and $SrFe_{12}O_{19}$) are promising materials for hard magnetic phase of ECC since they are affordable, chemically and thermally stable, and reveal high coercivity.[7] There are several reports[8–12] on successful preparation of hexaferrite-based ECCs combined with soft magnetic ferrites, especially Ni–Zn ferrite. However, the significant increase of magnetization could be achieved only by composing hexaferrites with ferromagnetic metals having higher saturation magnetization values, *e.g.* with iron, cobalt and alloys. Recently, Xu *et al.*[13] reported a self-assembly of $SrFe_{12}O_{19}$ submicron particles and cobalt nanoparticles into the core/shell exchange-coupled material. However, a distinct improvement in the magnetic properties of the composite compared to precursor phases was not achieved. The probable reason was a high initial aggregation of $SrFe_{12}O_{19}$ particles, which is a common problem of high-temperature methods for hexaferrite production.[14]

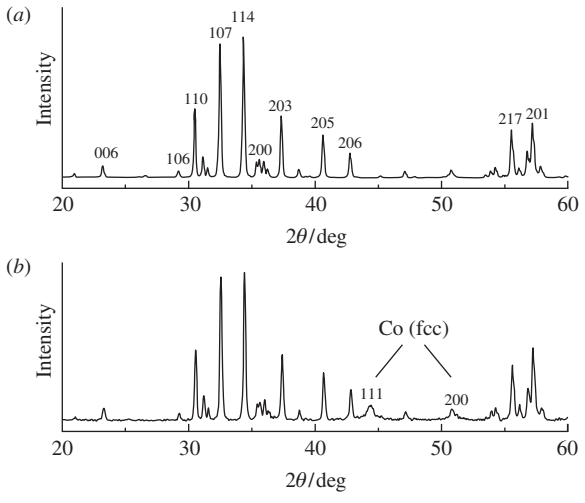

Figure 1 XRD patterns of (*a*) $SrFe_{10.7}Al_{1.3}O_{19}$ and (*b*) $SrFe_{10.7}Al_{1.3}O_{19}$/Co composite.

Herein, we report on the synthesis of hard-soft magnetic composite by coating low-aggregated hexaferrite particles with cobalt nanoparticles.

M-type hexaferrite particles with composition $SrFe_{10.7}Al_{1.3}O_{19}$ were obtained by glass crystallization† according to our previously reported procedure.[15] This is an efficient method to produce non-aggregated submicron hexaferrite particles with the high structural quality.[16–18]

Figure 1 shows XRD pattern‡ of the obtained powder, which represents the single phase hexaferrite.[19] The lattice parameters $a = 5.8472(3)$ and $c = 22.912(1)$ Å are lower in comparison with those[19] of $SrFe_{12}O_{19}$ ($a = 5.885$ and $c = 23.05$ Å), which indicates a partial substitution of aluminum by iron. The substitution degree in $SrFe_{12-x}Al_xO_{19}$ can be estimated as $x = 1.3$ according to the Vegard's law for solid solutions.[20] The obtained x value is

† The glass with nominal composition of $13\,SrO–5.5\,Fe_2O_3–4.5Al_2O_3–4B_2O_3$ was prepared by melting the mixture of $SrCO_3$, H_3BO_3, Al_2O_3, and Fe_2O_3 in a platinum crucible at 1300 °C and fast quenching the melt between two steel rollers. Subsequently, the glass was annealed at 950 °C for 24 h. The hexaferrite particles were separated by dissolving the borate matrix in 3% HCl solution. All operations were performed in air atmosphere.

‡ X-ray diffraction (XRD) spectra of the samples were recorded on a Rigaku D/MAX 2500 diffractometer with CuKα radiation.

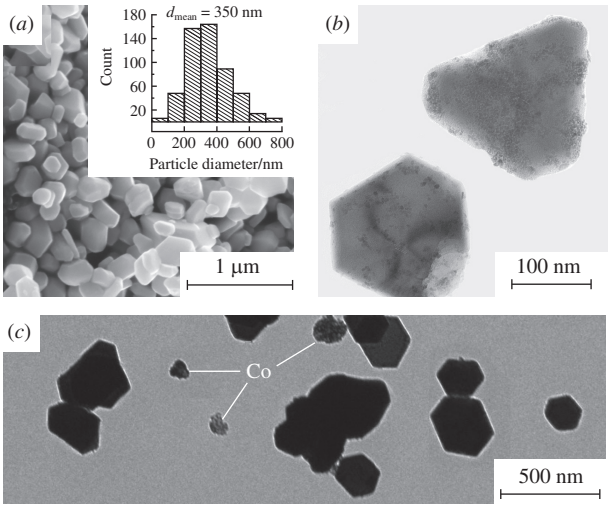

Figure 2 (*a*) SEM image of $SrFe_{10.7}Al_{1.3}O_{19}$ powder, inset shows the distribution of particles diameter (mean diameter of 350 nm); (*b*) TEM image of the hexaferrite particles covered by Co nanoparticles; (*c*) TEM image of cobalt agglomerates and hexaferrite particles in $SrFe_{10.7}Al_{1.3}O_{19}$/Co composite.

also consistent with the results of EDX analysis. According to the scanning electron microscopy (SEM),§ a mean diameter of hexaferrite particles of 350 nm [inset in Figure 2(*a*)], which is lower than 500 nm, a minimum size of magnetic domain for hexaferrites,[21] indicating the single-domain material in the sample.

The XRD pattern of the composite obtained¶ (see Figure 1) demonstrates that it consists of hexaferrite and fcc cobalt crystal phases,[24] while cobalt oxide phases were not observed. The broadening of cobalt diffraction peaks seems to be due to a small particles size.

Transmission electron microscopy (TEM) image†† of $SrFe_{10.7}Al_{1.3}O_{19}$/Co composite [Figure 2(*b*)] shows that the individual hexaferrite particles are covered by cobalt nanoparticles with mean diameter of 8 nm. Apparently, such a decoration of hexaferrite particles can be explained by the heterogeneous nucleation of cobalt nanoparticles on the hexaferrite surface, which corresponds to one of the reported mechanisms for metal salts reduction by ethylene glycol on oxide substrates.[25] In contrast to the homogeneous nucleation in the solution volume with subsequent agglomeration, the heterogeneous nucleation results in a better contact between hard and soft magnetic phases, which is essential for the exchange coupling. Moreover, the non-aggregated state of the hexaferrite particles provides a higher surface area for the cobalt deposition.

The observed composite microstructure has to provide an effective exchange-coupling between cobalt nanoparticles and hexaferrite. According to Skomski's theory of ECC, the size of soft phase should be less than twice of domain wall width (d_W) of hard magnetic phase.[1–3] For $SrFe_{12}O_{19}$, d_W of ~14 nm[5] and the cobalt particles mean diameter of 8 nm should fulfill this requirement.

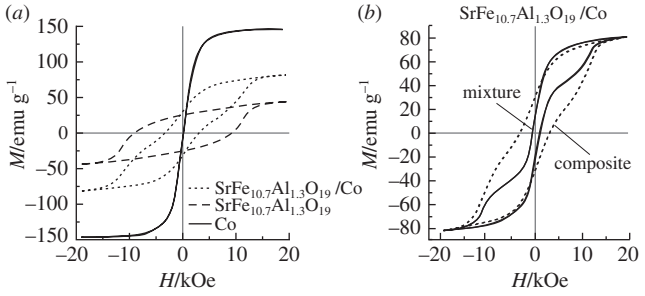

Figure 3 (*a*) Magnetic hysteresis loops of cobalt, hexaferrite and composite; (*b*) magnetic hysteresis loops of $SrFe_{10.7}Al_{1.3}O_{19}$/Co composite and a mechanical mixture of $SrFe_{10.7}Al_{1.3}O_{19}$ (68 wt%) and Co (32 wt%).

The *M vs. H* curves of the cobalt nanoparticles, the hexaferrite powder, and the composite measured at room temperature with original Faraday balance magnetometer are shown in Figure 3(*a*). The cobalt nanopowder is characterized by the low coercivity (H_c) of 140 Oe and high saturation magnetization (M_s) of 146 emu g^{-1}, which is slightly lower than that reported for bulk cobalt (164 emu g^{-1}).[26] The depressed magnetization value is probably related to the low particle size. The coercivity of $SrFe_{10.7}Al_{1.3}O_{19}$ (9.3 kOe) is 1.4 times higher than the largest known value for non-substituted $SrFe_{12}O_{19}$ (6700 Oe),[27] while the M_s value is reduced to 48 emu g^{-1} in comparison with $SrFe_{12}O_{19}$ (74 emu g^{-1} for monocrystals and about 65 emu g^{-1} for fine particles[21]) as expected for partial replacement of iron atoms by aluminum.[18] The shape of hexaferrite hysteresis loop is typical of randomly oriented single-domain Stoner–Wohlfarth particles with M_r/M_s ratio of 0.5.[28]

The magnetization curves of both the $SrFe_{10.7}Al_{1.3}O_{19}$/Co composite and its mechanical mixture are shown in Figure 3(*b*). In spite of the same cobalt particle diameter of 8 nm, the magnetization hysteresis of the mixture has a typical shape of two-phase material representing a significant narrowing at low fields. The composite demonstrates a substantially wider hysteresis, which is a result of exchange coupling between the components. The $SrFe_{10.7}Al_{1.3}O_{19}$/Co composite displays significantly higher M_S value of 80 emu g^{-1} than the initial hexaferrite. The composite also shows a higher remanence of 31 emu g^{-1} *vs.* 25 emu g^{-1} for the hard ferrite phase. However, H_c is reduced from 9.3 to 3.8 kOe. The decrease of the coercivity with the magnetization growth is a common phenomenon for all the hard-magnet materials as well as ECC.[5,28]

The hysteresis loop of the composite has still a low field narrowing, reflecting the incomplete coupling.[2] Obviously, a part of cobalt nanoparticles is not bound to the hexaferrite surface that is observed in Figure 2(*c*). This may happen due to a homogeneous cobalt nucleation with subsequent agglomeration resulting in a contaminated soft magnetic phase in the composite. The mass percentage of the phases in the material may be calculated according to the formula[5] $M_s^c = (1 - \alpha)M_s^h + \alpha M_s^s$, wherein the M_s^c, M_s^h, and M_s^s are the saturation magnetization values of composite, hard phase, and soft phase, respectively, and α is the mass fraction of soft phase. The estimated mass fraction of cobalt is 32%, which is definitely higher than expected from TEM micrographs. Therefore, the presence of non-coupled cobalt particles is very probable. Despite this impurity, the composite reveals higher M_r and H_c than the prepared mixture of cobalt and hexaferrite particles with the same phase content. Thus, the used technique allows one to obtain the hard ferrite/cobalt composite with the exchange-coupling effect, however some optimization of

§ SEM was performed using a LEO Supra 50 VP microscope.

¶ Hexaferrite powder (0.1 g) was ultrasonically dispersed in ethylene glycol (60 ml). Sodium acetate (1 g), sodium hydroxide (4 g), and cobalt(II) chloride hexahydrate (0.576 g) were added to the prepared suspension. The mixture was heated up to 100 °C for 1 h in air atmosphere to dissolve all the chemicals under mechanical stirring. Subsequently, the temperature was increased to 180 °C and held for 1 h to reduce Co^{2+} ions into metallic cobalt. The mechanisms of dissolution and reduction of cobalt ions by ethylene glycol are described in ref. 22. The solution was cooled down to room temperature; the product was separated with a magnet and washed three times with ethanol. At the final step, the obtained powder was annealed at 250 °C for 30 min under argon atmosphere to improve cobalt crystallinity and magnetization[23] and remove residual organic compounds. To produce a reference material, the same synthetic procedure was applied for the preparation of pure cobalt sample. The mechanical mixture of hexaferrite and cobalt powders was also prepared by grinding in the agate mortar.

†† TEM was performed using a LEO 912 AB Omega microscope.

synthesis conditions is required to avoid homogeneous nucleation of cobalt.

In conclusion, we accomplished the synthesis of new magnetic composite consisted of Al-substituted hexaferrite submicron particles as the hard core and cobalt nanoparticles as the soft magnetic shell displaying the exchange-coupling effect. The synthesis was based on heterogeneous nucleation of cobalt on the surface of non-agglomerated hexaferrite particles during the process of the Co^{2+} reduction by ethylene glycol. This simple method is a promising way to enhance the magnetic properties of hexaferrite materials by the effective exchange-coupling with soft metallic phases.

This work was supported by the Russian Foundation for Basic Research (grant no. 15-03-04277).

References

1 K. J. Strnat and R. M. W. Strnat, in *Handbook of Magnetic Materials* (*Ferromagnetic Materials*), eds. E. P. Wohlfarth and K. H. J. Buschow, Elsevier, Amsterdam, 1988, vol. 4, pp. 134–204.
2 E. F. Kneller and R. Hawig, *IEEE Trans. Magn.*, 1991, **27**, 3588.
3 R. Skomski and J. M. Coey, *Phys. Rev. B*, 1993, **48**, 15812.
4 T. Schrefl, H. Kronmüller and J. Fidler, *J. Magn. Magn. Mater.*, 1993, **127**, 273.
5 A. López-Ortega, M. Estarder, G. Salazar-Alvarez, A. G. Roca and J. Nogués, *Phys. Rep.*, 2015, **553**, 1.
6 H. Zeng, J. Li, J. P. Liu, Z. L. Wang and S. Sun, *Nature*, 2002, **420**, 395.
7 R. C. Pullar, *Prog. Mater. Sci.*, 2012, **57**, 1191.
8 A. D. Volodchenkov, Y. Kodera and J. E. Garay, *J. Mater. Chem. C*, 2016, **4**, 5593.
9 L. Zhang and Z. Li, *J. Alloys Compd.*, 2009, **469**, 422.
10 A. Xia, C. Zuo, L. Zhang, C. Cao, Y. Deng, W. Xu, M. Xie, S. Ran, C. Jin and X. Liu, *J. Phys. D: Appl. Phys.*, 2014, **47**, 415004.
11 K. W. Moon, S. G. Cho, Y. H. Choa, K. H. Kim and J. Kim, *Phys. Status Solidi A*, 2007, **204**, 4141.
12 P. Jing, J. Du, J. Wang, J. Wei, L. Pan, J. Li and Q. Liu, *Sci. Rep.*, 2015, **5**, 15089.
13 X. Xu, J. Park, Y.-K. Hong and A. M. Lane, *Mater. Chem. Phys.*, 2015, **152**, 9.
14 L. A. Trusov, E. A. Gorbachev, V. A. Lebedev, A. E. Sleptsova, I. V. Roslyakov, E. S. Kozlyakova, A. V. Vasiliev, R. E. Dinnebier, M. Jansen and P. E. Kazin, *Chem. Commun.*, 2018, **54**, 479.
15 P. E. Kazin, L. A. Trusov, D. D. Zaitsev, Yu. D. Tretyakov and M. Jansen, *J. Magn. Magn. Mater.*, 2008, **320**, 1068.
16 P. E. Kazin, L. A. Trusov, D. D. Zaitsev and Yu. D. Tretyakov, *Russ. J. Inorg. Chem.*, 2009, **54**, 2081.
17 P. E. Kazin, L. A. Trusov, S. E. Kushnir, N. V. Yaroshinskaya, N. A. Petrov and M. Jansen, *J. Phys. Conf. Ser.*, 2010, **200**, 072048.
18 L. A. Trusov, A. V. Vasiliev, M. R. Lukatskaya, D. D. Zaytsev, M. Jansen and P. E. Kazin, *Chem. Commun.*, 2014, **50**, 14581.
19 X. Obradors, X. Solans, A. Collomb, D. Samaras, J. Rodriguez, M. Pernet and M. Font-Altaba, *J. Solid State Chem.*, 1988, **72**, 218.
20 N. J. Shirtcliffe, S. Thompson, E. S. O'Keefe, S. Appleton and C. C. Perry, *Mater. Res. Bull.*, 2007, **42**, 281.
21 T. Koutzarova, S. Kolev, C. Ghelev, K. Grigorov and I. Nedkov, in *Advances in Nanoscale Magnetism*, eds. B. Aktas and F. Mikailov, Springer, Berlin, Heidelberg, 2009, pp. 183–203.
22 T. Matsumoto, K. Takahashi, K. Kitagishi, K. Shinoda, J. L. Cuya Huaman, J.-Y. Piquemal and B. Jeyadevan, *New J. Chem.*, 2015, **39**, 5008.
23 G. S. Chaubey, C. Barcena, N. Poudyal, C. Rong, J. Gao, S. Sun and J. P. Liu, *J. Am. Chem. Soc.*, 2007, **129**, 7214.
24 J. Häglund, A. F. Guillermet, G. Grimvall and M. Körling, *Phys. Rev. B*, 1993, **48**, 11685.
25 E. A. Anumol, P. Kundu, P. A. Deshpande, G. Madras and N. Ravishankar, *ACS Nano*, 2011, **5**, 8049.
26 R. J. Pauthenet, *J. Appl. Phys.,* 1982, **53**, 8187.
27 K. Haneda, C. Miyakawa and K. Goto, *IEEE Trans. Magn.*, 1987, **23**, 3134.
28 E. C. Stoner and E. P. Wohlfarth, *Philos. Trans. R. Soc. London, Ser. A*, 1948, **240**, 599.

Received: 27th November 2017; Com. 17/5419